

Supporting Information

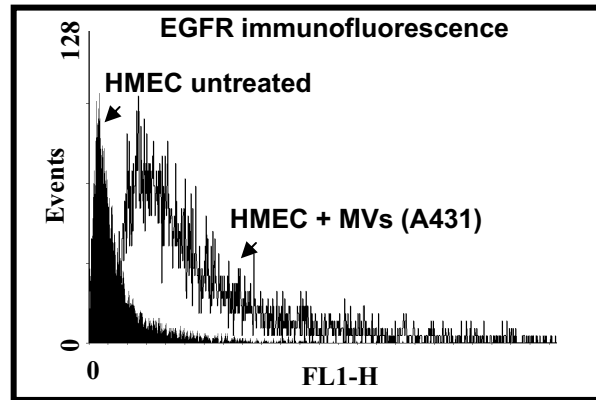
Al-Nedawi *et al.* 10.1073/pnas.0804543106

SI Methods

Protein Analysis. The cells and their corresponding MVs were lysed in the lysis buffer containing 10 mM Tris, pH 6.8, 5 mM EDTA, 50 mM NaF, 30 mM sodium pyrophosphate, 2% (wt/vol) SDS, 1 mM PMSF, and 1 mM Na_3VO_4 , for 10 min on ice, and proteins were resolved by SDS/PAGE (10% gels). Upon transfer, the membranes were immunoblotted with sheep anti-human EGFR, β -actin, and flotillin-1 antibodies, followed by incubation with appropriate HRP-conjugated secondary antibodies and chemiluminescence-plus reagents (enhanced chemoluminescence kit; Amersham Pharmacia). Blots were scanned and bands quantified using a Storm 860 scanner (GE Healthcare). Responses of HUVEC cells to MVs were detected upon plating 2×10^5 cells/mL followed by serum starvation for 24 h (DMEM 0.5% FBS) and overnight stimulation with MV preparations. MVs were either intact or preincubated with annexin-V, Diannexin, or CI-1033 as indicated, 1 h before their addition to the target

cells and under appropriate buffer conditions. In particular, for annexin V and Diannexin treatment, MVs were suspended in a minimum volume of annexin-binding buffer containing optimized levels of calcium ions (0.1 M Hepes, pH 7.4; 1.4 M NaCl; 25 mM CaCl_2). These agents were removed from the MV preparation by extensive washing before contact with HUVECs. Anti-phospho-Erk1/2 and anti-phospho-Akt antibodies (Cell Signaling Technologies) were used, as per supplier's recommendations. The signals were quantified using Image Quant and normalized to the total Erk1/2 and Akt, respectively. HUVEC lysates were incubated with anti-*p*-Tyr monoclonal antibody (PY20) for 3 h, immunoprecipitated using protein-G Sepharose (Sigma), and resolved on 10% SDS-polyacrylamide gels. Upon transfer, the membranes were probed with anti-VEGFR-2 monoclonal antibodies and developed using an enhanced chemoluminescence kit (Amersham Pharmacia Biotech).

A MV-mediated transfer of tumor cell derived EGFR to human microvascular endothelial cells (HMEC)



B Expression of VEGF in HMEC exposed to EGFR-containing MVs

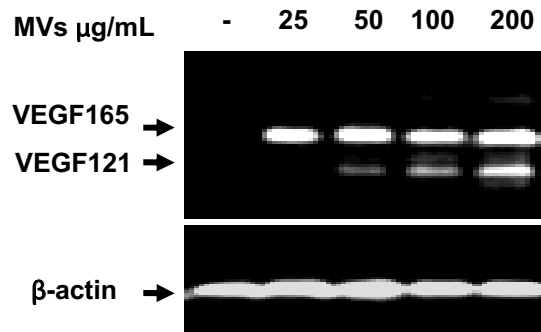


Fig. S1. (A) Immunodetection (FACS) of EGFR on the surface of human microvascular endothelial cells (HMECs) incubated with MVs derived from A431 cancer cells expressing oncogenic EGFR (compare Fig. 1 A and C). Untreated HMECs are EGFR-negative in this assay. (B). Induction of VEGF mRNA in HMECs exposed to EGFR-containing MVs. VEGF121 is less abundant in this case, and the expression is clearly dose-dependent (compare Fig. 3 B and C).

MV-mediated transfer of tumor cell derived EGFR to endothelial cells

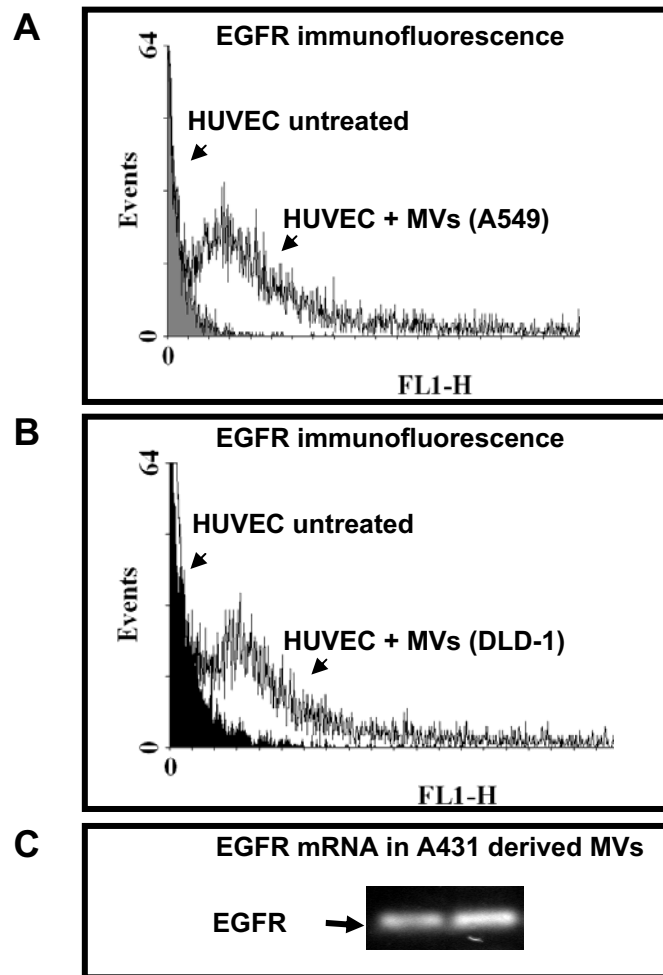


Fig. S2. (A and B) Immunodetection (FACS) of EGFR on the surface of endothelial cells (HUVECs) incubated with MVs derived from 2 different cancer cell lines expressing EGFR (compare Fig. 1A). Untreated HUVECs are EGFR-negative in this assay. (A) Lung cancer cell line A549 as donor of MV-related EGFR to HUVECs. (B) Colorectal cancer cell line DLD-1 as donor of MV-related EGFR. (C) MVs derived from A431 cells contain both EGFR protein (Fig. 1A) and mRNA (RT-PCR, as described in *Materials and Methods* in the main text).

MV-mediated transfer of tumor cell-derived EGFR triggers VEGFR-2 phosphorylation in endothelial cells

HUVECs exposed to EGFR containing MVs

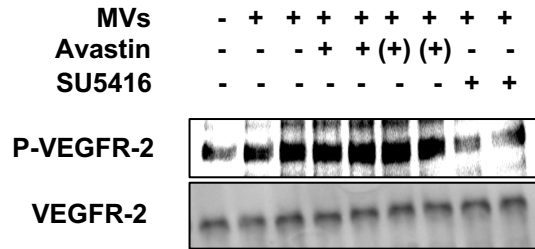


Fig. S4. Immunoprecipitate of phospho-VEGFR-2. The analysis was carried out on endothelial cells (HUVECs) exposed to EGFR-containing MVs, which were produced by A431 cancer cells. Uptake of these MVs leads to the expression of autocrine VEGF and phosphorylation of VEGFR-2 (Fig. 3D). This effect is inhibited by small-molecule VEGFR-2 inhibitor (SU5416), but not by the action of Avastin/bevacizumab, a neutralizing antibody that binds to VEGF. Unlike SU5416, bevacizumab would only block extracellular access of VEGF to VEGFR-2. The respective inhibitors were added either to HUVEC cells before addition of MVs (+), or to MVs before treatment of HUVECs (+). Bevacizumab was used at concentrations of 10 $\mu\text{g}/\text{mL}$ and 100 $\mu\text{g}/\text{mL}$, whereas SU5416 was used at 0.4 μM and 0.8 μM , both of which were effective (see *Materials and Methods* in the main text).

**Quantification of VEGFR2 phosphorylation
in HUVEC cells treated with
EGFR-containing MVs**

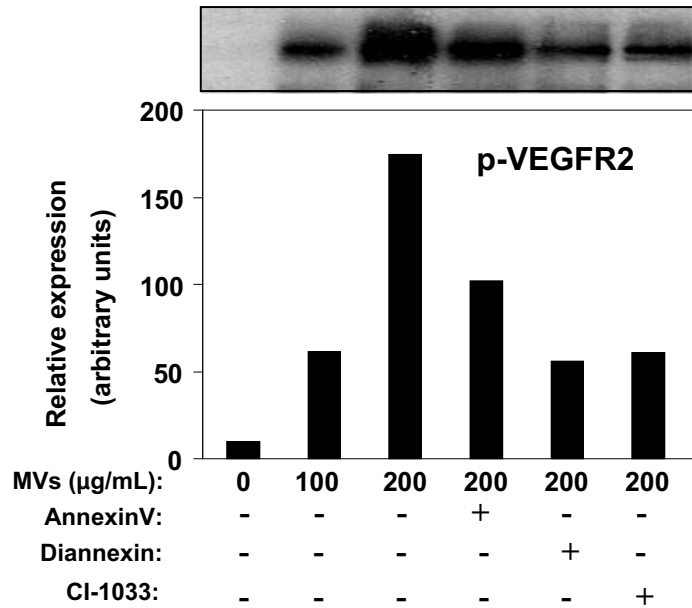


Fig. S5. Quantification that complements the content of Fig. 3D. The blots were subjected to densitometry scanning and results expressed as arbitrary units of optical density. As described for Fig. 3D and in *SI Methods*, starved HUVECs were treated with MV preparations incubated with annexin V, Diannexin, or CI-1033. PY20 antibody was used to immunoprecipitate the lysates and the resulting blots were probed for VEGFR2.

Detection of human EGFR on blood vessels in A431 Xenografts

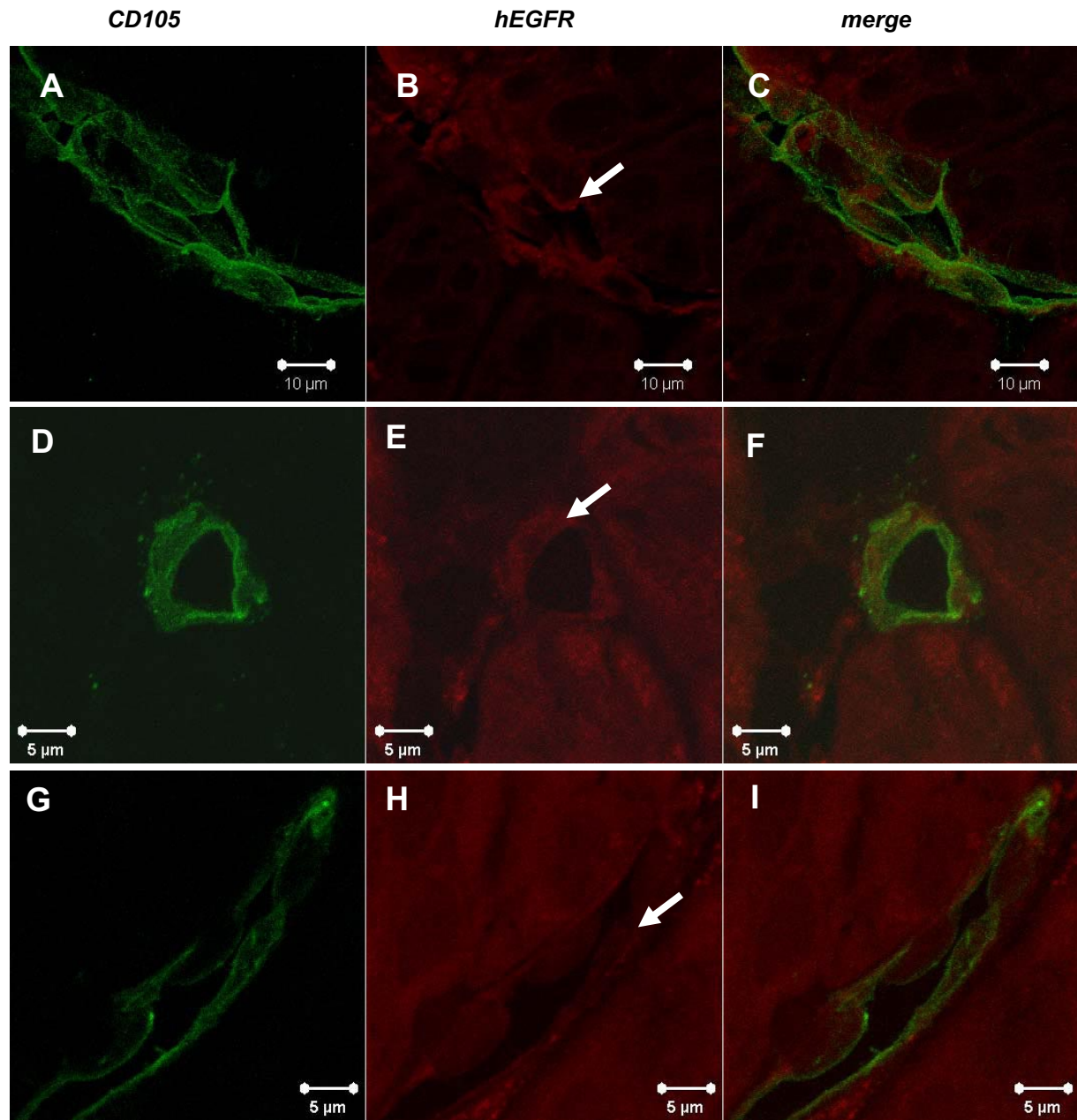


Fig. S7. Distinctive staining of tumor-associated endothelial cells (green) with tumor cell-derived hEGFR (red; arrows). Immunofluorescence of human A431 xenografts in SCID mice for endothelial markers (CD105; green; *A*, *D*, and *G*) and human EGFR (hEGFR; red; *B*, *E*, and *H*). Confocal images of several areas in tumors in which blood vessels were readily detectable have been collected using separate fluorescence channels, as indicated. Their automatic merger (*C*, *F*, and *I*) shows that hEGFR signal can be detected on endothelial cells positive for CD105. Anti-EGFR antibody used reacts exclusively with human EGFR (hEGFR; Cell Signaling Technologies no. 4405, clone 15F8) as in Fig. 1. High-resolution stacks and their 3D rotation are included as [SI Movies 1–3](#).

Detection of human P-EGFR on blood vessels in A431 Xenografts

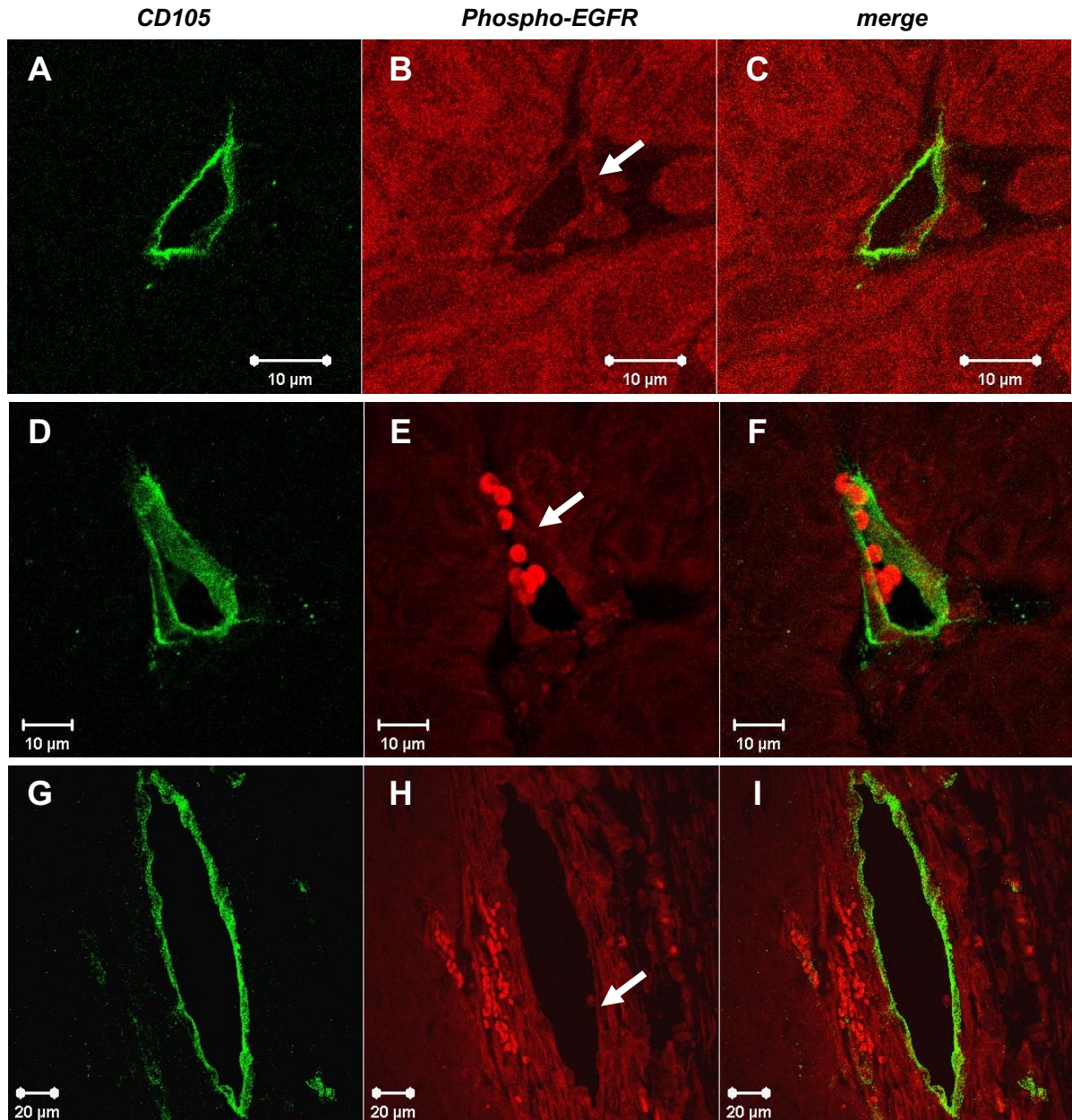
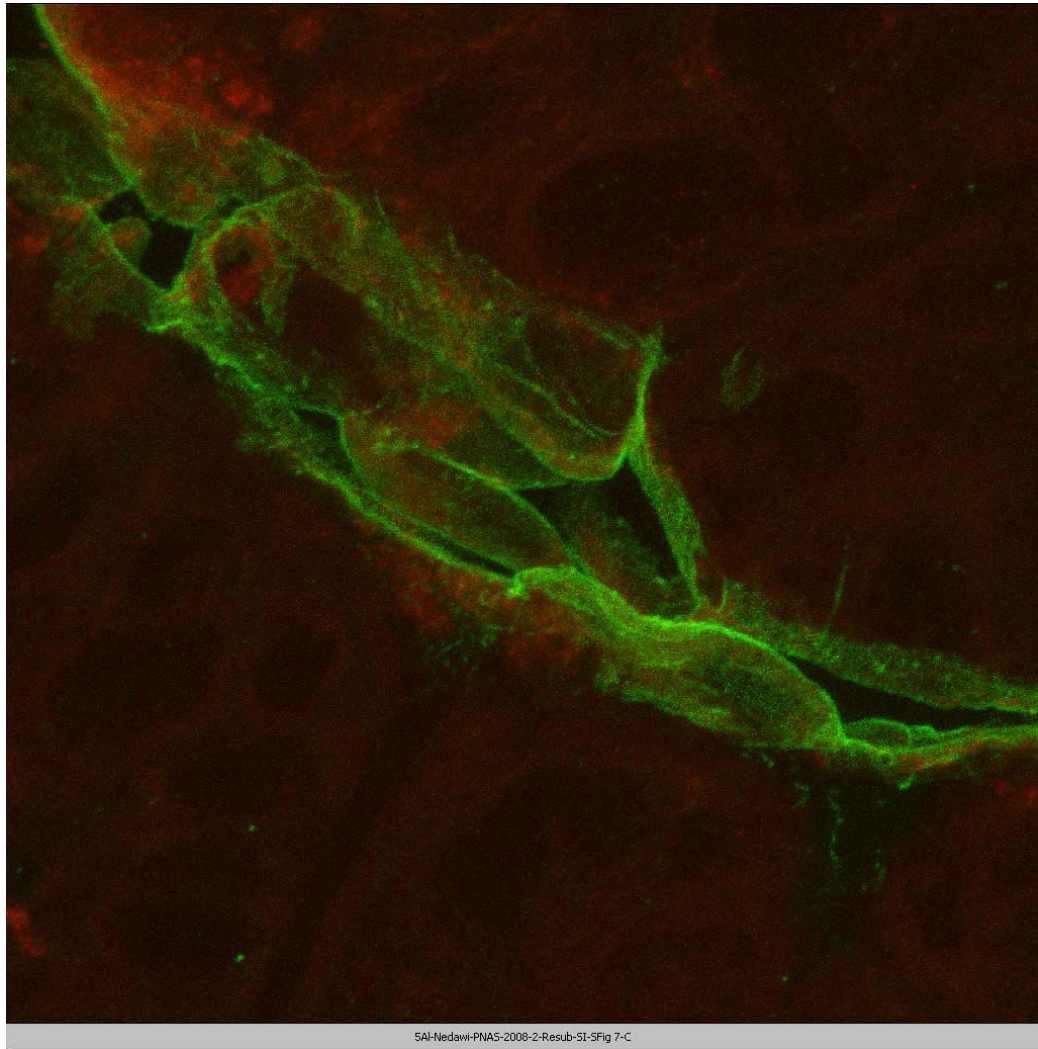
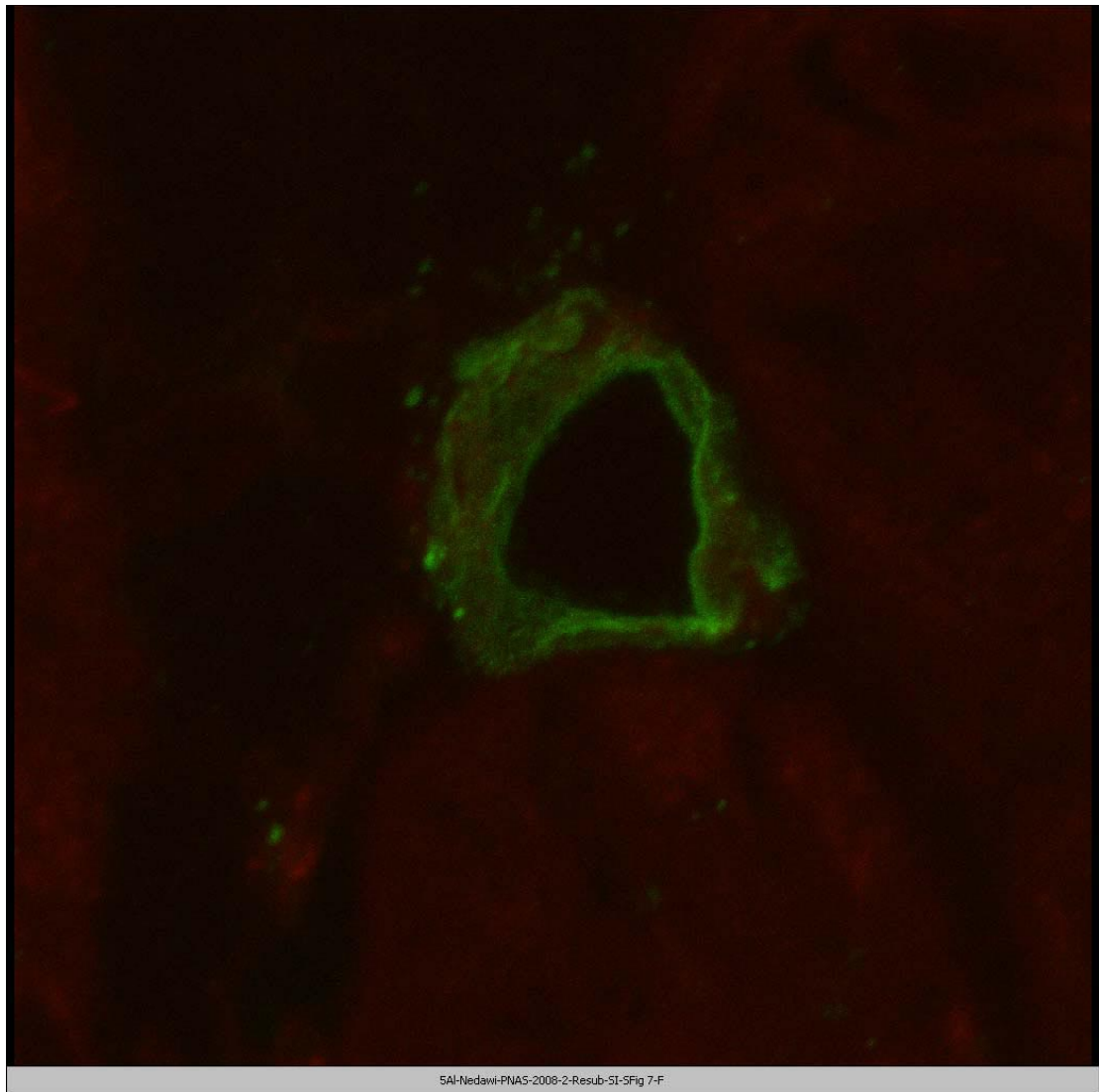


Fig. S8. Tumor-associated endothelial cells (green) stain for tumor cell derived phospho-EGFR (red; arrows). Human A431 xenografts were grown in SCID mice and processed for immunofluorescence using antibodies against endothelial markers (CD105; green; *A*, *D*, and *G*) and phospho-EGFR (P-EGFR; red; *B*, *E*, and *H*). Confocal images were collected using separate fluorescence channels, as indicated, and merged automatically using microscope software (*C*, *F*, and *I*). P-EGFR signal intensity differed between separate fields and specimens, likely indicating a heterogeneous expression of this antigen, whereas CD105 staining was relatively uniform. Red blood cells exhibited unspecific staining of A431 tumor xenografts for the host (mouse) endothelial cell-specific CD105 antigen (green) and tumor-derived (human) EGFR antigen (red) (compare [Fig. S7 A–C](#)) were visualized within the corresponding fluorescence channels. Several images were collected under high (*A–F*) and low power (*G–I*). P-EGFR signal is readily detected on endothelial cells positive for CD105, as in [Fig. 1](#). High-resolution stacks and their 3D rotation are included as [Movies 1–3](#)



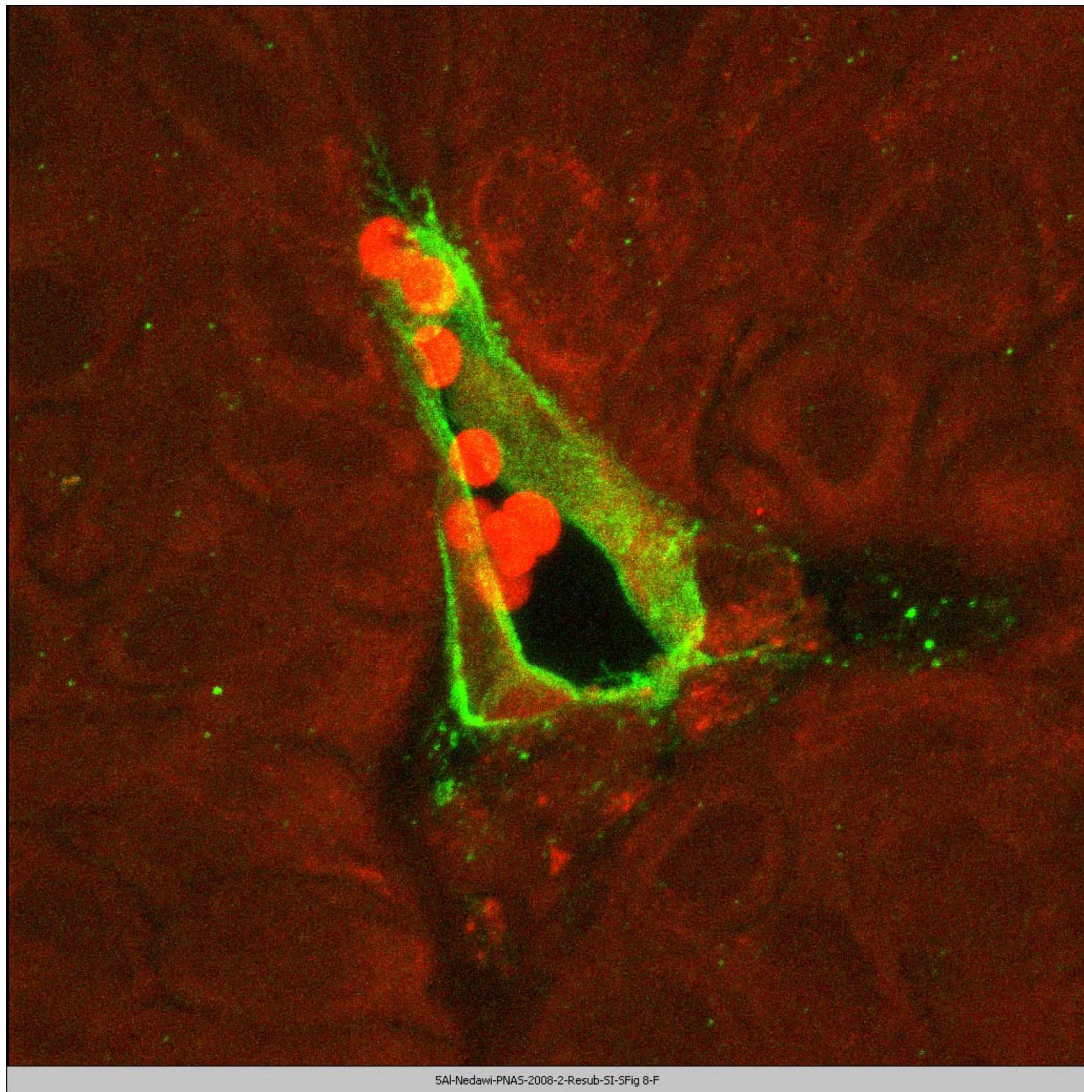
Movie S1. A431 tumor xenograft. Staining of the host (mouse) endothelial cells for CD105 (green) and tumor-derived (human) EGFR (red) (compare [Fig. S7 A-C](#)).

[Movie S1 \(AVI\)](#)



Movie S2. A431 tumor xenograft. Staining of the host (mouse) endothelial cells for CD105 (green) and tumor-derived (human) EGFR (red) (compare [Fig. S7 D–F](#)).

[Movie S2 \(AVI\)](#)



Movie S3. A431 tumor xenograft. Staining of the host (mouse) endothelial cells for CD105 (green) and tumor-derived (human) P-EGFR (red) (compare [Fig. S8 D-F](#)).

[Movie S3 \(AVI\)](#)